OFFICE OF NAVAL RESEARCH

Contract N00014-82K-0612

Task No. NR 627-838

TECHNICAL REPORT NO. 45

X-Ray Photoelectron Spectroscopy and Catalytic Activity of α-Zirconium Phosphate and Zirconium Phosphate

by

Jorge L. Colón. Deepak S. Thakur, Chao-Yeuh Yang,
Abraham Clearfield, and Charles R. Martin

Prepared for publication

in

The Journal of Catalysis

Department of Chemistry
Texas A&M University
College Station, TX 77843

February 2, 1990

REPORT DOCUMENTATION PAGE

Form Approved
OMB No. 0704-0188

1a. REPORT SECURITY CLASSIFICATION UNCLASSIFIED	1b. RESTRICTIVE MARKINGS
2a. SECURITY CLASSIFICATION AUTHORITY	3. DISTRIBUTION/AVAILABILITY OF REPORT APPROVED FOR PUBLIC DISTRIBUTION,
2b. DECLASSIFICATION/DOWNGRADING SCHEDULE	DISTRIBUTION UNLIMITED.
4. PERFORMING ORGANIZATION REPORT NUMBER(S) ONR TECHNICAL REPORT # 45	5. MONITORING ORGANIZATION REPORT NUMBER(S)
6a. NAME OF PERFORMING ORGANIZATION Dr. Charles R. Martin Department of Chemistry 6b. OFFICE SYMBOL (If applicable)	7a. NAME OF MONITORING ORGANIZATION Office of Naval Research
6c. ADDRESS (City, State, and ZIP Code) Texas A&M University College Station, TX 77843-3255	7b. ADDRESS (City, State, and ZIP Code) 800 North Quincy Street Arlington, VA 22217
8a. NAME OF FUNDING/SPONSORING ORGANIZATION Office of Naval Research 8b. OFFICE SYMBOL (If applicable)	9. PROCUREMENT INSTRUMENT IDENTIFICATION NUMBER Contract # N00014-82K-0612
8c. ADDRESS (City, State, and ZIP Code) 800 North Quincy Street Arlington, VA 22217	10. SOURCE OF FUNDING NUMBERS PROGRAM ELEMENT NO. / PROJECT NO. / TASK NO. / WORK UNIT ACCESSION NO.

11. TITLE (Include Security Classification)
X-Ray Photoelectron Spectroscopy and Catalytic Activity of α-Zirconium Phosphate and Zirconium Phosphate Sulfophenylphosphonate

12. PERSONAL AUTHOR(S)
Jorge L. Colón, Deepak S. Thakur, Chao-Yeuh Yang, Abraham Clearfield, and Charles R. Martin

13a. TYPE OF REPORT	13b. TIME COVERED	14. DATE OF REPORT (Year, Month, Day)	15. PAGE COUNT
Technical	FROM _____ TO _____	(90,01,31) Jan. 31, 1990	

16. SUPPLEMENTARY NOTATION

17. COSATI CODES			18. SUBJECT TERMS (Continue on reverse if necessary and identify by block number)
FIELD	GROUP	SUB-GROUP	X-ray photoelectron spectroscopic, α-zirconium phosphate, ZrP, zirconium phosphate sulfophenylphosphonate, $Ru(bpy)_3^{2+}$, catalytic, dehydration, cyclohexanol, alcohols, TRANSITION Metals

19. ABSTRACT (Continue on reverse if necessary and identify by block number)

X-ray photoelectron spectroscopic (XPS) analyses were performed on α-zirconium phosphate (ZrP) and on an organic derivative of ZrP, zirconium phosphate sulfophenylphosphonate (ZrPS). The XPS results show that the change of half of the phosphate groups in ZrP to sulfophenylphosphonate groups in ZrPS, changes the binding energy levels for some electrons in the solid. The XPS analyses also show that upon intercalation of $Ru(bpy)_3^{2+}$ into ZrPS, the binding energies of the ruthenium and nitrogen atoms of the metal complex are unperturbed relative to the free complex. ZrP samples show increased catalytic activity for dehydration of cyclohexanol with increased acidity of the sample. However, no correlation between Zr3d or Ols binding energies and catalytic activity was found.

ruthenium(2,2'-bipyridine)

20. DISTRIBUTION/AVAILABILITY OF ABSTRACT	21. ABSTRACT SECURITY CLASSIFICATION
☒ UNCLASSIFIED/UNLIMITED ☐ SAME AS RPT. ☐ DTIC USERS	UNCLASSIFIED
22a. NAME OF RESPONSIBLE INDIVIDUAL Dr. Robert Nowak	22b. TELEPHONE (Include Area Code) (202) 696-4410 / 22c. OFFICE SYMBOL

DD Form 1473, JUN 86 — Previous editions are obsolete. — SECURITY CLASSIFICATION OF THIS PAGE

X-RAY PHOTOELECTRON SPECTROSCOPY AND CATALYTIC ACTIVITY OF α-ZIRCONIUM PHOSPHATE AND ZIRCONIUM PHOSPHATE SULFOPHENYLPHOSPHONATE

Jorge L. Colón, Deepak S. Thakur, Chao-Yeuh Yang,

Abraham Clearfield,[1] and Charles R. Martin[1]

Department of Chemistry

Texas A&M University

College Station, Texas 77843

[1] To whom correspondence should be addressed.

ABSTRACT

X-ray photoelectron spectroscopic (XPS) analyses were performed on α-zirconium phosphate (ZrP) and on an organic derivative of ZrP, zirconium phosphate sulfophenylphosphonate (ZrPS). The XPS results show that the change of half of the phosphate groups in ZrP to sulfophenylphosphonate groups in ZrPS, changes the binding energy levels for some electrons in the solid. The XPS analyses also show that upon intercalation of $Ru(bpy)_3^{2+}$ into ZrPS, the binding energies of the ruthenium and nitrogen atoms of the metal complex are unperturbed relative to the free complex. ZrP samples show increased catalytic activity for dehydration of cyclohexanol with increased acidity of the sample. However, no correlation between Zr3d or O1s binding energies and catalytic activity was found.

Introduction

Zirconium phosphates (see Figure 1) are inorganic ion exchange materials with layered structures (*1*). α-Zirconium phosphate, $Zr(HPO_4)_2 \cdot H_2O$, (α-ZrP) is the most extensively characterized zirconium phosphate (*1-4*). α-ZrP is composed of layers of Zr atoms; the metal atoms lie nearly in a plane in a pseudohexagonal arrangement. Each Zr atom layer has bridging phosphate groups situated alternatively above and below the Zr atom plane (Figure 1A). Three oxygen atoms of each phosphate group are bonded to three different zirconium atoms; each zirconium atom is octahedrally coordinated by oxygen atoms. The fourth oxygen atom of the phosphate group bears an exchangeable proton. The solid is composed of stacks of these layers with an interlayer distance of 7.6 Å.

Organic derivatives of α-ZrP can be formed by replacing a fraction of the phosphate groups with phosphonate groups (*5-7*). These organic substituents are covalently attached to the phosphate groups of α-ZrP. These organic substituents increase the interlayer distance by protruding into the interlayer space. Yang and Clearfield have recently prepared a partially substituted phenylsulfonate derivative of α-ZrP (*8-10*). This organo-derivative of α-ZrP is called zirconium phosphate sulfophenylphosphonate, $Zr(HPO_4)(O_3P\text{-}C_6H_4SO_3H)$ (ZrPS). ZrPS has an interlayer space of 16.1 Å (Figure 1B) with a much larger interlayer volume than α-ZrP. Since the strongly hydrophilic SO_3H group promotes swelling, ZrPS forms colloids when exposed to aqueous solutions.

The primary objective of the studies reported here was to investigate the effect of the organo substituent on the electronic charge density of ZrP. X-ray photoelectron spectroscopy (XPS) should in principle be suited for

obtaining information on the chemical and physical state of the surface of these materials (*11*). We have used XPS to explore the relationship between organo substitution and electronic charge density. The results of these XPS studies are reported here.

In addition to this main objective, the work described here had several secondary objectives. First we have conducted XPS investigations of ZrPS which had been exchanged with the photocatalyst $Ru(bpy)_3^{2+}$ (bpy = 2,2'-bipyridine). The objective of these studies was to determine the effect of the chemical microenvironment within ZrPS on the structure and properties of $Ru(bpy)_3^{2+}$. The results of these investigations are also reported here.

Another objective was to evaluate the catalytic activity of zirconium phosphates (*12,13*). Zirconium phosphates are acidic catalysts. The acid catalyzed decomposition of alcohols has been used as a test reaction for related systems (*14-16*). In our earlier work (*12,13*), we showed that the catalytic activity of zirconium phosphates is related to the number and acidic strength of the hydroxyl groups present on the surface. However, Vinek et al. (*17*) have suggested that the catalytic activity of several phosphates can be related to the oxygen 1s binding energy of the catalysts. We were interested in determining whether this relationship is applicable to ZrP.

The final objective was, therefore, to determine whether XPS can be used to access the catalytic activity of ZrP samples. As part of these catalytic studies, we have conducted XPS investigations on catalytic ZrP samples. These investigations proved that, contrary to Vinek et al. results (*17*), there is no relationship between the O1s binding energy and the catalytic activity of the zirconium compounds. In addition, the effect of the crystallinity of the sample on the XPS data was elucidated. The results of these investigations of

the catalytic properties of zirconium phosphates are also reported in this paper.

Experimental Section

Materials. $Ru(bpy)_3Cl_2 \cdot 6H_2O$ was obtained from G. F. Smith and used as received. Water was either triply distilled or circulated through a Milli-Q water purification system (Millipore Corp.). All other reagents and solvents were of the highest available grade and were used without further purification.

Procedures. As noted in the introduction, one of the objectives of this work was to access the effect of crystallinity on the XPS binding energy of the Zr atom. Clearfield *et al.* (*18*) have shown that the extent of crystallinity in ZrP increases with the concentration of H_3PO_4 used in the synthesis and with the duration of refluxing during synthesis. Correspondingly, we prepared three batches of ZrP. The first was prepared with 0.5 M H_3PO_4 and was refluxed for 48 hours. These conditions yielded noncrystalline ZrP (labeled here ZrP-0.5:48). The second batch of ZrP was prepared with 4.5 M H_3PO_4 and was refluxed for 48 hours. These conditions yielded semicrystalline ZrP (labeled here ZrP-4.5:48). The final batch was prepared with 12 M H_3PO_4 and was refluxed for 336 hours. These conditions yielded highly crystalline ZrP (ZrP-12:336).

The organic derivative of ZrP (ZrPS = $Zr(HPO_4)(O_3P\text{-}C_6H_4SO_3H)$, Figure 1B) was prepared as described previously (*8*). $Ru(bpy)_3^{2+}$ was incorporated (loaded) into ZrPS as described previously (*9*). ZrPS samples for XPS analysis were prepared either as KBr pellets or as films on filter paper (*9*).

Catalytic Activity. The acid catalyzed dehydration of cyclohexanol was used to test the catalytic activity of the ZrP samples. This reaction yields

cyclohexene and water as the major products and cyclohexanone as a minor product. The amount of cyclohexanone was less than 0.5% for all the ZrP samples.

The catalytic activity for cyclohexanol dehydration was determined at 400°C in a continuous flow reactor pretreated as described elsewhere (*12,13*). The flow of the reactants was metered with a Sage syringe pump. Products were analyzed on a gas chromatography column packed with 10% OV-17 on 100/120 Chromosorb WHP. The quantity of cyclohexanol converted to cyclohexene was monitored as a function of contact time in the reactor; these data were analyzed via a pseudo first order rate expression. The catalytic activity is given as the first order rate constant.

Instrumentation. X-ray photoelectron spectroscopy (XPS) analyses of the ZrPS samples were performed at the Surface Science Facility at Texas A&M University by using a Kratos XSAM-800 spectrometer. Primary excitation was provided by a Mg anode biased at 12 kV with 20 mA of filament current. The spectra were collected by using a fixed analyzer transmission mode on a hemispherical electron analyzer. The binding energies for the spectra were referenced to the C 1s line, which was fixed at 285 eV.

For the catalytic experiments, XPS analyses of the zirconium compounds were performed on a Hewlett Packard 5950-A ESCA spectrometer. The excitation radiation was AlKα ($h\lambda$ = 1486.6 eV). The sample was gently ground under dry nitrogen inside a glove box and mounted onto the sample holder. The sample was allowed to outgas for 1 hr in the sample preparation chamber before introduction into the spectrometer. An electron flood gun was used to control charging effects. Sufficient scanning was used to obtain peak heights of at least 5K counts over the background; peak heights of 10-20K counts were

normally used. The decomposition of the peaks was performed using the XPS spectrometer's nonlinear least-squares decomposition software. The C 1s line at 285 eV was used as reference.

Results and Discussion

Comparison of Zirconium and Phosphorus XPS Data for ZrP and ZrPS. Figure 2 shows typical XPS spectra for free $Ru(bpy)_3^{2+}$, unexchanged ZrPS, and $Ru(bpy)_3^{2+}$-exchanged ZrPS. Tables 1, 2, and 3 show the core level binding energy values for different elements in the ZrPS and α-ZrP samples. The following discussion will explain the results for the different elements and compare these results to other reported XPS experiments of zirconium phosphates. First, the Zr3d binding energies of ZrPS will be compared with the corresponding binding energies for ZrP obtained from the literature (*19,20*) and from the present investigations. The objective of these comparisons is to elucidate the effect, if any, of the $-C_6H_4SO_3H$ substituent on the binding energy values of ZrPS.

Figure 3 shows the $Zr3d_{3/2}$ and $Zr3d_{5/2}$ region of the XPS spectra of ZrPS and Table 1 lists the binding energy data obtained from the peaks in Figure 3. The separation between the two Zr3d peaks in ZrPS is 2.3-2.4 eV. This peak separation is in good agreement with the Zr3d peak separation in ZrP (2.2-2.3 eV (*19*), 2.3-2.5 eV (*20*), and 2.3-2.6 eV, this work) and is characteristic of Zr(IV) compounds. This confirms that the ZrPS synthesis has yielded the layered acid phosphate of tetravalent zirconium (*8*); i.e., that the incorporation of the $-C_6H_4SO_3H$ group does not change the valence state of the zirconium atoms.

Figure 4 shows the XPS spectra of the Zr3d region for the various ZrP samples and for the other zirconium compounds investigated in this study;

Table 2 presents the binding energy data obtained from these spectra. The $Zr3d_{5/2}$ binding energies for ZrO_2, $Zr(SO_4)_2$, ZrP-0.5:48 (noncrystalline), and ZrP-12:36 (highly crystalline) are identical, (184.2 eV) (Table 2); the binding energy for ZrP-4.5:48 (semicrystalline) is 0.8 eV higher. The same relationship is observed for the $Zr3d_{3/2}$ binding energies (186.6-186.8 eV for ZrO_2, $Zr(SO_4)_2$, ZrP-0.5:48, and ZrP-12:36; 187.5 eV for ZrP-4.5:48).

A comparison of the data in Tables 1 and 2 shows that the Zr3d binding energies of ZrP (Table 2) are higher than the Zr3d binding energies for ZrPS (Table 1). The reduced Zr3d binding energies observed for the ZrPS samples indicate a reduced polarization of the Zr-O bonds in ZrPS (*19*). We can minimize the effect of charging in the binding energy comparison by considering not only absolute, but also relative chemical shifts. The difference in photoelectron energies between two electrons in two different samples gives useful chemical shift information since charging effects cancel out in an energy difference. The $Zr3d_{5/2}$ - *O1s binding energy difference* in α-ZrP is 347.5 eV whereas in ZrPS the difference is 348.3 eV. This observation also suggest a reduced polarization of the Zr-O bond in ZrPS (*19*). ZrPS differs from ZrP in that half of the -OH groups in ZrP are replaced by $-C_6H_4SO_3H$ groups in ZrPS. Thus, substitution of -OH by $-C_6H_4SO_3H$ reduces the polarization of the Zr-O bond. This conclusion is corroborated by the phosphorus binding energy data (vide infra).

The phosphorus 2s and $2p_{3/2}$ binding energies for ZrP (Table 2) are higher than the corresponding binding energies for ZrPS (Table 1). Alberti *et al.* (*19*) compared the P2s binding energy of ZrP to the P2s binding energies for Fe, Al, and Ga phosphates; again, the ZrP binding energies were found to be higher. Alberti *et al.* (*19*) attributed the higher P2s binding energy in ZrP

to the increased polarity of the O-P bond in this compound. The O-P bond polarity is enhanced due to polarization induced by the proton bonded to the phosphorus atoms in ZrP.

The above analysis suggests that the reduced phosphorus binding energies for ZrPS relative to ZrP (Tables 1 and 2) is attributable to the diminution in O-P polarization associated with the replacement of -OH groups with $-C_6H_4SO_3H$ groups. The identical conclusion was reached through an analysis of the Zr3d binding energy data (vide supra). Again, to rule out any charging effects, we should compare binding energy differences. Alberti *et al.* (*19*) have suggested that the binding energy difference between P2s (or P2p) and O1s should be used when comparing binding energy values between phosphate-containing compounds.

The average P2s - O1s difference for ZrPS is 340.6 eV (Table 1); Alberti *et al.* (*19*) found a P2s - O1s difference of 340 eV for ZrP and a difference of 341.5 eV for Fe, Al, and Ga phosphates. A smaller P2s - O1s difference corresponds to a higher extent of polarization of the P-O bond. The ZrPS value is intermediate between that of ZrP and the trivalent phosphates, indicating an intermediate P-O polarization caused by the existence of both P-OH and $P-C_6H_4SO_3H$ groups in ZrPS.

Comparison of Oxygen XPS Data for ZrP and ZrPS. The Zr and P XPS data suggest that the Zr-O and P-O bonds are more polarized in ZrP than in ZrPS. What can the O1s XPS data from these compounds tell us about the charge distribution and chemical characteristics of these systems? Figure 5 shows that the O1s band for ZrPS is structured. The main peak is centered at 532.0 eV (Table 1); a shoulder (centered at 533.7 eV) occurs on the high binding energy side of the main peak. The main peak is attributed to the oxygens of the phosphate and sulfonate groups (*19-21*) (the sulfur 2p binding energy was also observed

in these samples). The shoulder is due to the -OH's bonded to phosphorus.

In contrast to the ZrPS samples, the O1s peak in ZrP must be resolved into three component peaks (Figure 6). The main peak is centered around 533 eV with a shoulder at higher binding energy and a smaller shoulder at lower binding energy. Alberti *et al.* (*19*) also found that the O1s peak of ZrP could be resolved into three component peaks. Alberti *et al.* (*19*) attributed the low energy shoulder to surface Zr-OH groups formed through hydrolytic reactions. This is corroborated by the fact that $Zr(OH)_4$ shows a O1s binding energy at lower energies than the zirconium phosphates (*19*). Since the ZrPS samples do not show the lower binding energy shoulder on the O1s band, hydrolytic reactions are not occurring in ZrPS. This conclusion is corroborated by the fact that IR spectra for ZrPS (*8*) do not show a vibrational peak characteristic of a Zr-OH group.

The binding energy of the O1s main peak in ZrPS is smaller than the O1s energy in ZrP (Figure 6 and Table 2). This reduction in O1s binding energy for ZrPS is again attributed to the replacement of -OH with $-C_6H_4SO_3H$ in half of the phosphate groups in ZrPS. However, we have pointed out above that the differences in Zr3d and P2s binding energies between ZrP and ZrPS are attributed to a higher Zr-O and P-O bond polarization in the ZrP samples. This interpretation suggests that the electronic charge density surrounding the oxygen atom should be greater in ZrP that in ZrPS. If this is true then we should have observed a lower O1s binding energy for ZrP (due to charge transfer) than for ZrPS; the opposite was observed. This apparent contradiction can be explained by taking into consideration the structure of ZrP and ZrPS.

A lower O1s binding energy in ZrP than in ZrPS is not observed because the charge transfer occurs over all the oxygens coordinated to the zirconium and the phosphorus. There are six oxygen atoms coordinated to the every Zr atom in ZrP. Therefore, the effect of any change in polarization will be felt entirely by the Zr atom whereas each of the oxygens coordinated to this Zr atom will only feel a partial change. The charge density change felt by each oxygen can be small enough as to be undetectable. This is why Alberti et al. did not observe any binding energy shift for O1s of ZrP relative to other phosphate compounds (*19*).

This polarization effect observed in ZrP (due to the relative number of Zr, P, and O atoms) should also be observed in ZrPS. However, in ZrPS only three oxygens are in the same coordination environment as the oxygens coordinated to Zr in ZrP. The three other oxygens in ZrPS are bonded to a phosphorus having a sulfophenylphosphonate substituent; this substituent is not present in ZrP. In addition, ZrPS has three oxygens as part of the sulfonate group in the sulfophenylphosphonate substituent. The binding energy of an O1s in a sulfonate group is about 532 eV (reference 21 and Table 2) which is exactly the O1s binding energy observed in our ZrPS samples. The different environment for oxygen in ZrPS compared to ZrP suggest that the lower O1s binding energy observed in ZrPS comes from the oxygens in the sulfonate group. The change in electronic charge density for the oxygens coordinated to Zr in ZrP is not big enough to shift its binding energy to lower values than in ZrPS.

It is important to point out that final state relaxation (*22*) can be ruled out as a contributor to these binding energy shifts. Final state relaxation would have affected these two related compounds (ZrP and ZrPS) to a

similar extent. In addition, final state relaxation occurs to a lesser extent in insulators than in metals (*22*). Therefore, our data indicate that the difference in Z-O and P-O bond polarization is the reason for the chemical shifts observed in the binding energies.

XPS Studies of $Ru(bpy)_3^{2+}$-exchanged ZrPS. The objective of the XPS studies of $Ru(bpy)_3^{2+}$-exchanged ZrPS was to elucidate the effect (if any) of the interlayer microenvironment on the intercalated $Ru(bpy)_3^{2+}$ counterion. We have previously reported the XPS spectra of $Ru(bpy)_3Cl_2$ and of $Ru(bpy)_3^{2+}$ exchanged into ZrPS samples (6.52% of the sulfonate sites were exchanged with $Ru(bpy)_3^{2+}$) (*6*). We present in Tables 1 and 3 binding energies for ZrPS samples containing a broad range of concentrations of $Ru(bpy)_3^{2+}$. All binding energy values were found to be independent of concentration of $Ru(bpy)_3^{2+}$ in ZrPS.

The binding energy for $Ru3d_{5/2}$ in $Ru(bpy)_3Cl_2$ is at 280.8 eV; the binding energy for $Ru3d_{5/2}$ in $Ru(bpy)_3^{2+}$ which has been incorporated into ZrPS is 280.9-281.2 eV. These values are in accord with literature values for $Ru(bpy)_3^{2+}$ and other Ru(II) compounds (*23-30*). The binding energy for a Ru(III) ion would be 2.3 eV more positive than that for a Ru(II) ion (*26,31*). Since our binding energy values are similar to those for other Ru(II) species, we can rule out any electronic modification (i.e. partial oxidation) of $Ru(bpy)_3^{2+}$ upon intercalation. In addition, the Zr3d binding energy values observed when $Ru(bpy)_3^{2+}$ is exchanged into ZrPS do not differ from the values for ZrPS which is devoid of $Ru(bpy)_3^{2+}$. Thus, the introduction of the metal complex into the interlayer space of ZrPS does not influence the electronic charge density of the zirconium atoms.

Table 3 indicates that the ZrPS which is devoid of $Ru(bpy)_3^{2+}$ shows a N1s XPS signal. This N1s signal arises from some unidentified impurity in ZrPS. This impurity is also present in the $Ru(bpy)_3^{2+}$-exchanged ZrPS samples (Table 3). The alternate explanation for the presence of the 402.1 eV peak in the $Ru(bpy)_3^{2+}$-exchanged samples is that protonation of a bpy ligand occurs within the interlayer space of ZrPS (*20,32,33*). We have previously reported results of careful infrared and UV-visible spectroscopic investigations of $Ru(bpy)_3^{2+}$-exchanged ZrPS (*9*). The intent of these investigations was to determine if evidence for protonation of a bpy ligand could be gathered. We found no evidence for protonation of the bpy's in $Ru(bpy)_3^{2+}$-exchanged ZrPS (*9*). Hence, the 402.1 XPS peak observed in these samples is due to an impurity.

Catalytic Studies. In recent years, it has been recognized that dehydration of alcohol requires both electron donor and electron acceptor sites (*14-16*). The strength of acidic and basic sites determines the catalytic activity and selectivity. Vinek *et al.* (*17*) and Noller and Kladning (34) have proposed that the XPS binding energy values for cationic and anionic sites can be used as a measure of acidity/basicity or electron pair accepting/donating (EPA or EPD) capability of a given catalytic compound. The increase in binding energy for a cationic site indicates an increase in its EPA strength, while the increase in binding energy for an anionic site indicates lower EPD strength.

Using a series of magnesium compounds as catalysts, Vinek *et al.* (*17*) have shown that magnesium phosphate, with higher magnesium 2p and oxygen 1s binding energy values, exhibit higher alcohol dehydration activity than other magnesium compounds with lower binding energy values. However, Davis *et al.* (*35*) found no correlation between the alcohol dehydration activity of several metal oxide catalysts and O1s binding energy. We have performed cyclohexanol

dehydration activity and XPS measurements on a series of catalytic ZrP samples. The idea was to determine whether there exists a correlation between the O1s binding energy of the ZrP samples and the catalytic activity, as suggested by Vinek *et al.* (*17*). This study should indicate whether XPS data from ZrP samples can be used to access the catalytic activity of ZrP compounds.

The conversion of cyclohexanol to cyclohexene at 400°C as a function of time was measured for each of the catalysts. Figure 8 presents first order plots of the cyclohexanol dehydration activity data for the various zirconium compounds. The first order rate constants for cyclohexanol dehydration for the various catalysts were evaluated using the kinetic expression (*12,13*):

$$-[2\ln(1-x) + x] = kt \qquad (1)$$

where x is the fractional conversion, k is the first order rate constant, and t is the contact time in minutes, given by the ratio of the weight of the catalyst (g) to the flow rate (g/min). The slopes of the straight lines in Figure 8 yield the values of the specific reaction rate constants k (min^{-1}). Dehydrogenation to cyclohexanone was less than 0.5 wt% for the zirconium samples. These results indicate that these phosphates are selective towards cyclohexene formation.

The dehydration activity data in Figure 8 shows the following trend: ZrP-4.5:48 (semicrystalline) > ZrP-12:336 (highly crystalline) > ZrP-0.5:48 (noncrystalline). However, the activity relationship can be expressed on a per surface area basis by dividing the rate constant by the surface area - ZrP-4.5:48 (34.6 m^2/g), ZrP-12:336 (1.8 m^2/g), and ZrP-0.5:48 (2.7 m^2/g). On

a per surface area basis the activities are:

ZrP-12:336	>	ZrP-0.5:48	>	ZrP-4.5:48
(0.50 g min^{-1} m^{-2})		(0.14 g min^{-1} m^{-2})		(0.082 g min^{-1} m^{-2})

Therefore, ZrP-12:336 has the highest activity per unit surface area.

An attempt was made to correlate the $Zr3d_{5/2}$ and O1s binding energies for various samples with their catalytic activity. Figure 9 shows plots of rate constant vs. XPS binding energy. Although ZrP-0.5:48 (noncrystalline) and ZrP-12:336 (highly crystalline) have the same Zr3d binding energy (Table 2), ZrP-12:336 is 3 times more active than ZrP-0.5:48 (Figure 9A). In addition, ZrP-4.5:48 has the highest Zr3d binding energy, but the smallest activity. Similarly, the three phosphate samples have comparable O1s binding energies, but their catalytic activities differ markedly (Figure 9B). These results indicate that, contrary to the results of Vinek et al., no correlation exist between binding energy and catalytic activity.

Based on these results no clear correlation between catalytic activity and XPS binding energy can be established. Similar conclusions were reached by Davis *et al.* (*35*) in their catalytic activity investigations by XPS O1s binding energy studies. These results are reasonable since only one out of four oxygens in the phosphate group bears a proton and XPS analyzes only about 30 Å into the bulk of the material. Therefore, the oxygens present in these surface -OH groups do not change the overall binding energy of the main oxygen 1s signal. In fact, the phosphate samples with differing acidities have almost identical O1s binding energy. In conclusion, XPS cannot be used to access the catalytic activity of these phosphate samples.

Our previous measurements indicate that catalytic activity for cyclohexanol dehydration depends upon the number and strength of acid sites on the catalyst surface at 400°C (*12,13*). For example, ZrP-0.5:48 (noncrystalline) loses most of its surface hydroxyl groups due to excessive dehydroxylation at this temperature, whereas ZrP-4.5:48 (semicrystalline) and ZrP-12:336 (highly crystalline) exhibit maxima at 400°C in the acid strength versus calcination temperature curve. The difference in their catalytic activity should, then, be related to the surface hydroxyl groups (*12*).

Conclusions

This study has demonstrated that XPS can give some information about the chemical environment in layered zirconium phosphate and its organic derivatives. The comparison made between the XPS binding energies observed in the ZrPS samples and in the ZrP samples have shown that ZrPS and ZrP have similar electronic properties. The binding energy differences between ZrP and ZrPS result from the influence of $-C_6H_4SO_3H$ groups in ZrPS (absent in ZrP) on the polarization of the bonds in the material. The environment in ZrPS also does not promote any hydrolytic reactions of the Zr atoms.

The environment in ZrPS has no effect on the nature of the intercalated $Ru(bpy)_3^{2+}$ complex. The binding energies for Ru(II) and bipyridine nitrogen are not affected upon intercalation. No evidence for protonation of the bpy's in $Ru(bpy)_3^{2+}$-exchanged ZrPS is observed. In addition, the binding energies in $Ru(bpy)_3^{2+}$-exchanged ZrPS are independent of concentration of $Ru(bpy)_3^{2+}$ in ZrPS.

No correlation between XPS O1s binding energy and catalytic activity was observed for ZrP. Recently, La Ginestra, *et al.* (*36*) reported catalytic activity measurements for the dehydration of isopropanol and 1- and 2-butanol,

and the isomerization of 1-butene in α-ZrP. In accord with our conclusions (*12,13*), these authors suggest that the active centers in α-ZrP are the Brønsted sites on the surface. The interlayer region is not involved in the catalytic activity of these materials. The strength of the acidic sites increase upon heating above 350°C. This transformation probably occurs through partial or total transformation of hydrogen phosphate to P-O-P groups with progressive formation of a layered pyrophosphate phase (*36,37*).

A small amount of activity is due to a second site (*12,13,36*) which is responsible for the residual catalytic activity observed in the alcohol dehydration on Cs^+-ZrP. La Ginestra *et al.* (*36*) have suggested that this residual catalytic activity can be due to new Brønsted sites generated either from the crumbling of the crystallites after interaction with water, or from some Cs^+ diffusion into the exchanger and consequent migration of H^+ on the surface. Clearfield and Thakur (*12*) have suggested that the residual catalytic activity comes from some Lewis sites, associated with the zirconium atoms or with defects caused by hydrolysis of HPO_4^{2-} groups, which are not poisonable by Cs^+ ions.

Acknowledgements. Financial support for this work was provided by the Robert A. Welch Foundation, the Office of Naval Research, and the Air Force Office of Scientific Research. J.L.C. acknowledges the support from the Texas A&M University Minority Merit Fellowship.

References

1. Clearfield, A., *in* "Inorganic Ion Exchange Materials" (A. Clearfield, Ed.). CRC Press, Boca Raton, Fla., 1982.

2. Alberti, G., *Acc. Chem. Res.* 11, 163 (1978).

3. Clearfield, A., and Thakur, D. S., *Appl. Catal.* 26, 1 (1986).

4. Clearfield, A., *Chem. Rev.* 88, 125 (1988).

5. Alberti, G., Constantino, U., Allulli, S., and Tomassini, N., *J. Inorg. Nucl. Chem.* 40, 1113 (1978).

6. Dines, M. B., and DiGiacomo, P. M., *Inorg. Chem.* 20, 92 (1981).

7. Alberti, G., in "Recent Developments in Ion Exchange" (P. A. Williams, and M. J. Hudson, Eds.), pp 233-248. Elsevier Applied Science, London, 1987.

8. Yang, C.-Y., and Clearfield, A., *React. Polym., Ion Exch., Sorbents* 5, 13 (1987).

9. Colón, J. L., Yang, C.-Y., Clearfield, A., and Martin, C. R., *J. Phys. Chem.* 92, 5777 (1988).

10. Colón, J. L., Yang, C.-Y., Clearfield, A., and Martin, C. R., submitted to *J. Phys. Chem.*

11. Delgass, W. N., Haller, G. L., Kellerman, R., and Lunsford, J. H., "Spectroscopy in Heterogeneous Catalysis", Chap. 8. Academic Press, New York, 1979.

12. Clearfield, A., and Thakur, D. S., *J. Catal.* 65, 185 (1980).

13. Thakur, D. S., and Clearfield, A., *J. Catal.* 69, 230 (1981).

14. Winfield, M. E., *in* "Catalysis" (P. H. Emmett, Ed.), Vol. VII, p.93. Reinhold, New York, 1960.

15. Pines, H., and Manassen, J., *Adv. Catal.* 16, 49 (1966).

16. Kibby, C. L., Lande, S. S., and Hall, W. K., *J. Am. Chem. Soc.* 94, 214 (1972).

17. Vinek, H., Noller, H., Ebel, M., and Schwarz, K., *J. Chem. Soc. Faraday Trans. I* 73, 734 (1977).

18. Clearfield, A., Oskarsson, A., and Oskarsson, C., *Ion Exch. Membr.* 1, 91 (1972).

19. Alberti, G., Constantino, U., Marletta, G., Puglisi, O., and Pignataro, S., *J. Inorg. Nucl. Chem.* 43, 3329 (1981).

20. Mattogno, G., Ferragina, C., Massucci, M., Patrono, P., and La Ginestra, A., *J. Electron Spectrosc. Relat. Phenom.* 46, 285 (1988).

21. Lindberg, B. J., Hamrin, K., Johansson, G., Gelius, U., Fahlman, A., Nordling, C., and Siegbahn, K., *Physica Scripta* 1, 286 (1970).

22. Briggs, D., and Seah, M. P. "Practical Surface Analysis". Wiley, London, 1989.

23. De Wilde, W., Peeters, G., and Lunsford, J. H., *J. Phys. Chem.* 84, 2306 (1980).

24. Abdo, S., Canesson, P., Cruz, M., Fripiat, J. J., and Van Damme, H., *J. Phys. Chem.* 85, 797 (1981).

25. Weaver, T. R., Meyer, T. J., Adeyemi, S. A., Brown, G. M., Eckberg, R. P., Hatfield, W. E., Johnson, E. C., Murray, R. W., and Untereker, D., *J. Am. Chem. Soc.* 97, 3039 (1975).

26. Citrin, P. H., *J. Am. Chem. Soc.* 95, 6472 (1973).

27. Brant, P., and Stephenson, T. A., *Inorg. Chem.* 26, 22 (1987).

28. Lane, B. C., Lester, J. E., and Basolo, F., *J. Chem. Soc., Chem. Commun.* 1618 (1971).

29. Abruña, H. D., Meyer, T. J., and Murray, R. W., *Inorg. Chem.* 18, 3233 (1979).

30. Shpiro, E. S., Antoshin, G. V., Tkachenko, O. P., Gudkov, S. V., Romanovsky, B. V., and Minachev, Kh. M., *in* "Structure and Reactivity of Modified Zeolites" (P. A. Jacobs, N. I. Jaeger, P. Jiru, G. Schulzekloff, and V. B. Kazansky, Eds.), Studies in Surface Science and Catalysis, Vol. 18, pp.31-39. Elsevier, Amsterdam, 1984.

31. Citrin, P. H., and Ginsberg, A. P., *J. Am. Chem. Soc.* 103, 3673 (1981).

32. Defosse, C., and Canesson, P., *React. Kinet. Catal. Lett.* 3, 161 (1975).

33. Canesson, P., Cruz, M. I., and Van Damme, H., *in* "International Clay Conference 1978" (M. M. Mortland, and V. C. Farmer, Eds.), Developments in Sedimentology No. 27, pp. 217- 225. Elsevier, Amsterdam, 1979.

34. Noller, H., and Kladning, K., *Catal. Rev. Sci. Eng.* 13, 194 (1976).

35. Davis, B. H., Russell, S. N., Reucroft, P. J., and Shalvoy, R. B., *J. Chem. Soc., Faraday Trans. I*, 76, 1917 (1980).

36. La Ginestra, A., Patrono, P., Berardelli, M. L., Galli, P., Ferragina, C., and Massucci, M. A., *J. Catal.* 103, 346 (1987).

37. Segawa, K., Kurusu, Y., Nakajima, Y., and Kinoshita, M., *J. Catal.* 94, 491 (1985).

Table 1

Zirconium, Phosphorus, Oxygen, and Sulfur Binding Energies for ZrPS and $Ru(bpy)_3^{2+}$-Exchanged ZrPS

	Binding Energies, eV[a,b]					
$Ru(bpy)_3^{2+}$, %[c]	$Zr3d_{3/2}$	$Zr3d_{5/2}$	P2s	$P2p_{3/2}$	O1s	$S2p_{3/2}$
0%	186.1	183.7	191.5	134.1	532.0 533.7	169.0
1.74%	185.9	183.5	191.3	134.1	531.9 533.5	-----
4.34%	185.9	183.5	191.4	133.9	531.7 533.5	168.9
6.52%	185.8	183.4	191.1	134.0	531.8 533.4	168.9
13.04%	186.0	183.6	191.3	133.9	532.0 533.5	168.8
15.20%	185.8	183.5	191.2	-----	531.6 532.9	-----
21.75%	186.0	183.6	191.2	133.9	531.8 533.4	168.7

[a] The binding energies are referenced to the C 1s line, which was fixed at 285 eV.

[b] For electrons with two B.E. values the decomposition of the corresponding peaks was performed with a nonlinear least squares program of the spectrometer software (Autofit command in Peak Synthesis).

[c] Percent of $-SO_3^-$ sites in ZrPS occupied by $Ru(bpy)_3^{2+}$.

Table 2

Zirconium 3d, Oxygen 1s, and Phosphorus 2s Binding Energies for Various Catalytic Zirconium Compounds.

	Binding Energies, eV			
Compound	$Zr3d_{3/2}$	$Zr3d_{5/2}$	O1s	P2s
ZrO_2 (monoclinic)	186.8	184.2	530.9	----
$Zr(SO_4)_2$ (anhyd)	186.6	184.2	532.0	----
α-ZrP(0.5:48)	186.6	184.2	532.9	192.0
α-ZrP(4.5:48)	187.5	185.0	533.3	192.8
α-ZrP(12:336)	186.6	184.2	533.0	192.0
α-ZrP[a] (hydrated)	187.8	185.5	533.3	193.4
α-ZrP[a] (dehydrated)	188.1	185.9	533.4	193.8
γ-ZrP[a] (hydrated)	187.3	185.0	532.7	193.0

[a] Reference 19.

Table 3

Ruthenium 3d and Nitrogen 1s Binding Energies for $Ru(bpy)_3^{2+}$-Exchanged ZrPS

	Binding Energies, eV[a,b]	
$Ru(bpy)_3^{2+}$, %[c]	$Ru3d_{5/2}$	N1s
$Ru(bpy)_3Cl_2$	280.8	399.9
0%	-----	402.1
1.74%	281.2	399.8 402.2
4.34%	-----	----- 401.1
6.52%	281.1	400.4 402.1
13.04%	281.0	400.2 402.0
15.20%	281.0	400.2 402.2
21.75%	280.9	400.2 402.1

[a] The binding energies are referenced to the C 1s line, which was fixed at 285 eV.

[b] For electrons with two B.E. values the decomposition of the corresponding peaks was performed with a nonlinear least squares program of the spectrometer software (Autofit command in Peak Synthesis).

[c] Percent of $-SO_3^-$ sites in ZrPS occupied by $Ru(bpy)_3^{2+}$.

Figure 1. Idealized structure of (A) α-ZrP and (B) ZrPS.

Figure 2. X-ray photoelectron spectra of (A) $Ru(bpy)_3Cl_2$, (B) ZrPS, and (C) $Ru(bpy)_3^{2+}$-exchanged ZrPS.

Figure 3. X-ray photoelectron spectra of (A) ZrPS (P2s, $Zr3d_{3/2}$, and $Zr3d_{5/2}$ binding energy region), (B) Least squares fit to Zr3d binding energy region, and (C) Zr3d peak decomposition.

Figure 4. Zirconium 3d binding energy region of the XPS spectra of α-ZrP samples, $Zr(SO_4)_2$, and ZrO_2.

Figure 5. (A) X-ray photoelectron spectra of ZrPS O1s binding energy region, (B) Least squares fit to O1s binding energy region, and (C) O1s peak decomposition.

Figure 6. Oxygen 1s region of the XPS spectra of α-ZrP samples, $Zr(SO_4)_2$, and ZrO_2. Dashed curve shows decomposition of the O1s peak for the ZrP 0.5:48 sample.

Figure 7. X-ray photoelectron spectra showing the N1s binding energy region of (A) $Ru(bpy)_3Cl_2$, (B) ZrPS, and (C) $Ru(bpy)_3^{2+}$-exchanged ZrPS.

Figure 8. First order plots of the cyclohexanol dehydration activity of ZrP samples of varying crystallinity at 400°C.

Figure 9. Variation of dehydration rate constant with (A) Zr3d binding energy and (B) O1s binding energy for ZrP samples.

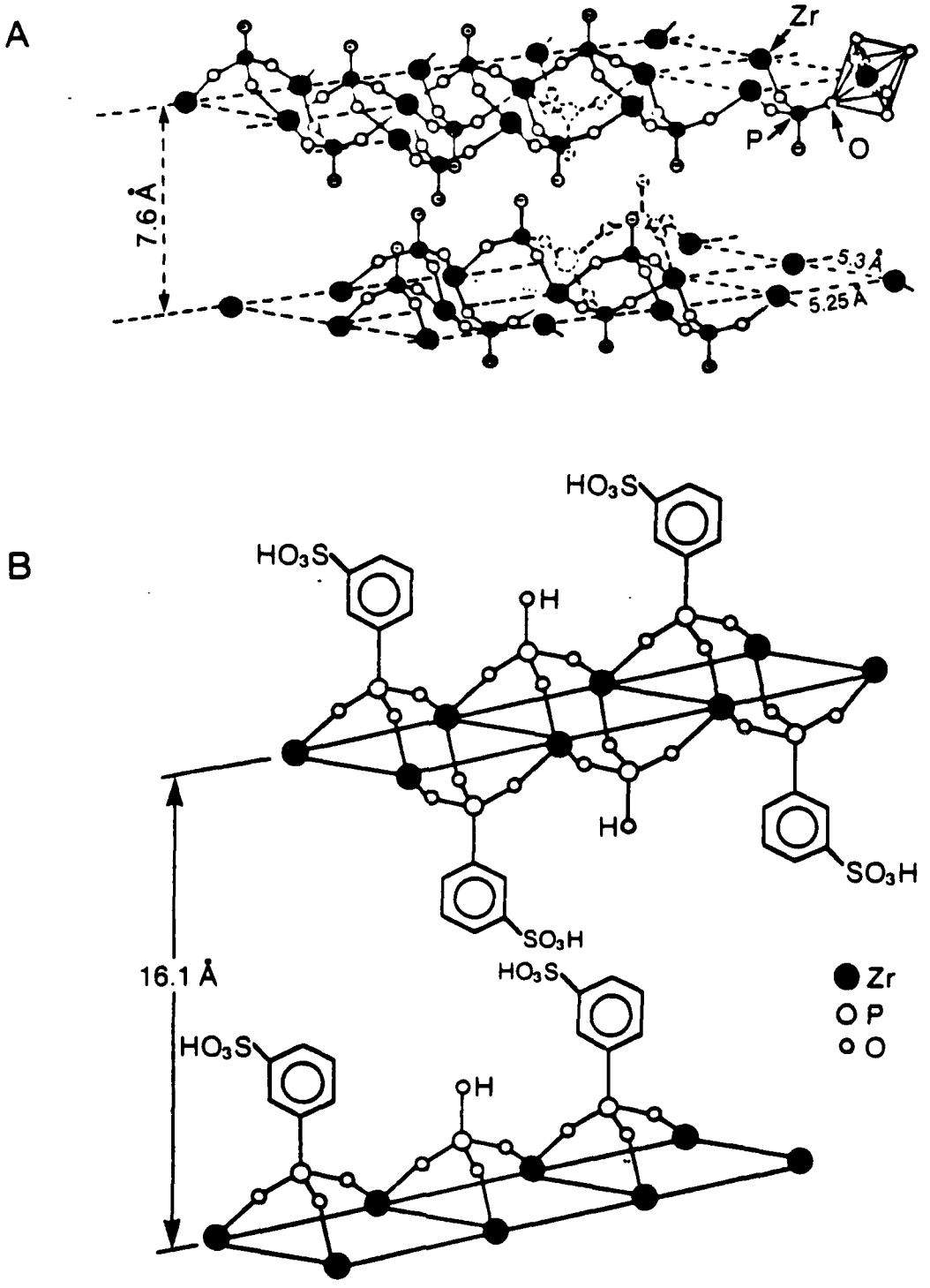

Figure 1

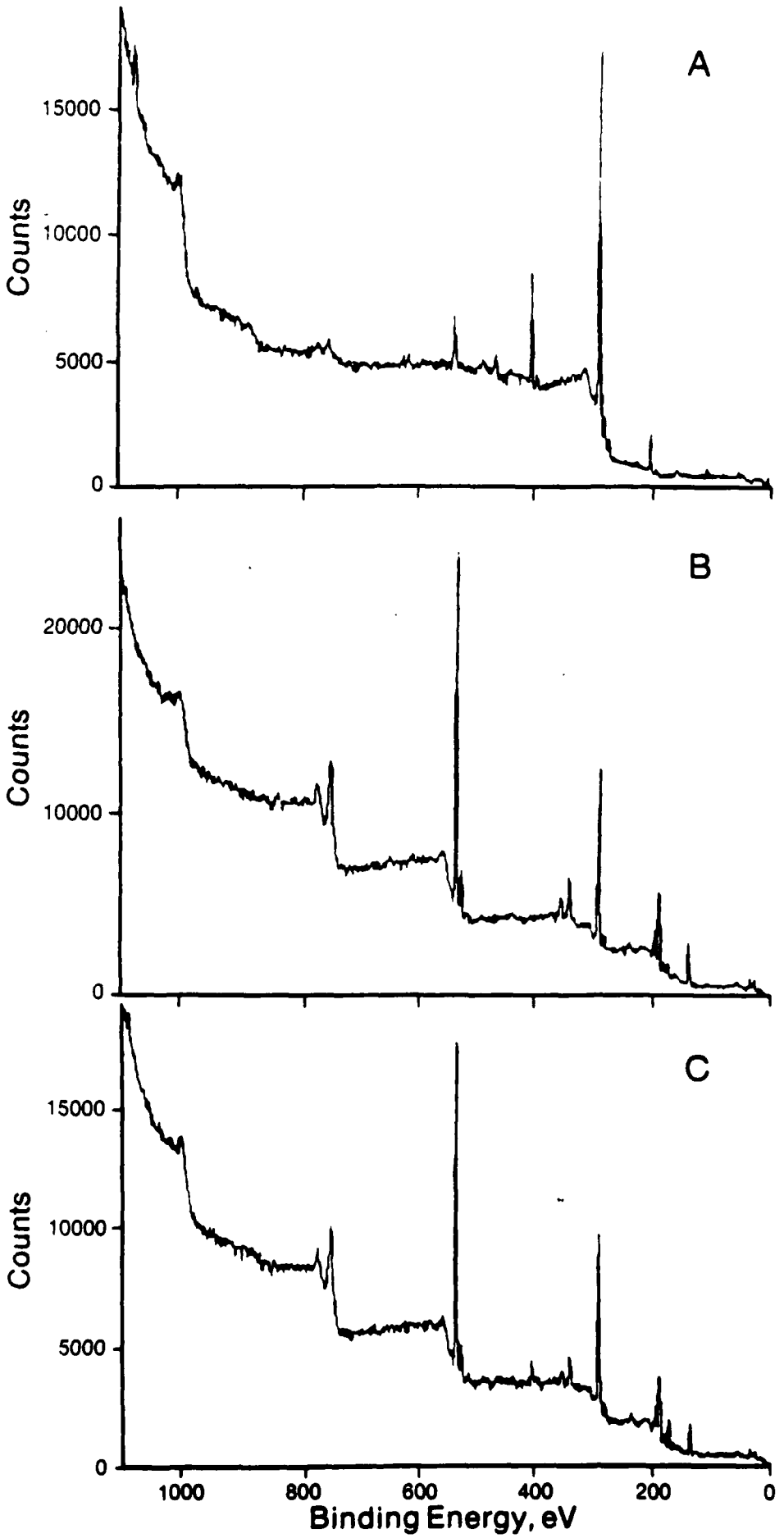
A
B
C
Counts
15000
10000
5000
0
20000
1000
800
600
400
200
Binding Energy, eV

Figure 2

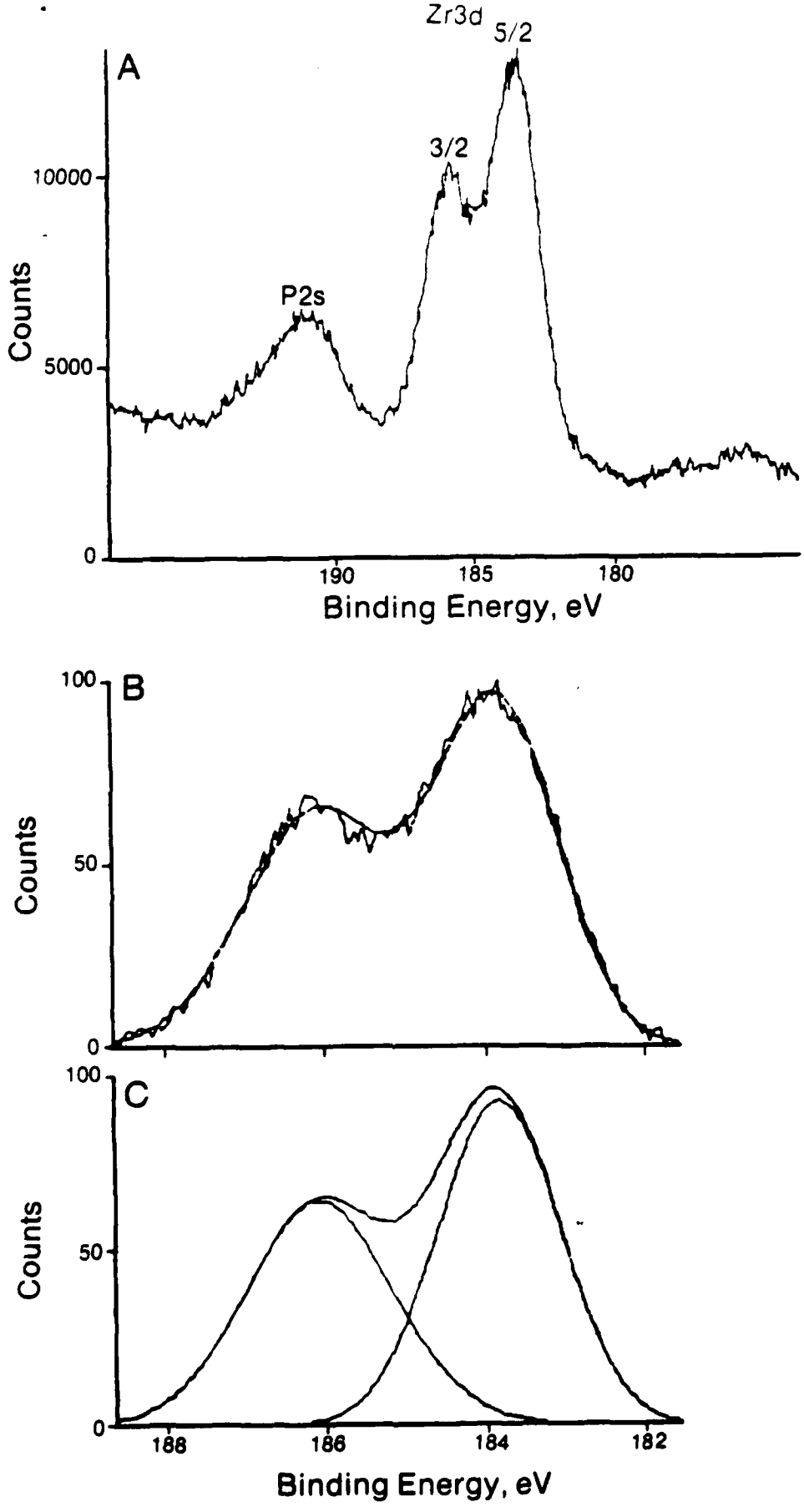
A
Zr3d
5/2
3/2
P2s
10000
5000
0
Counts
190
185
180
Binding Energy, eV
B
100
50
0
Counts
C
100
50
0
Counts
188
186
184
182
Binding Energy, eV

Figure 3

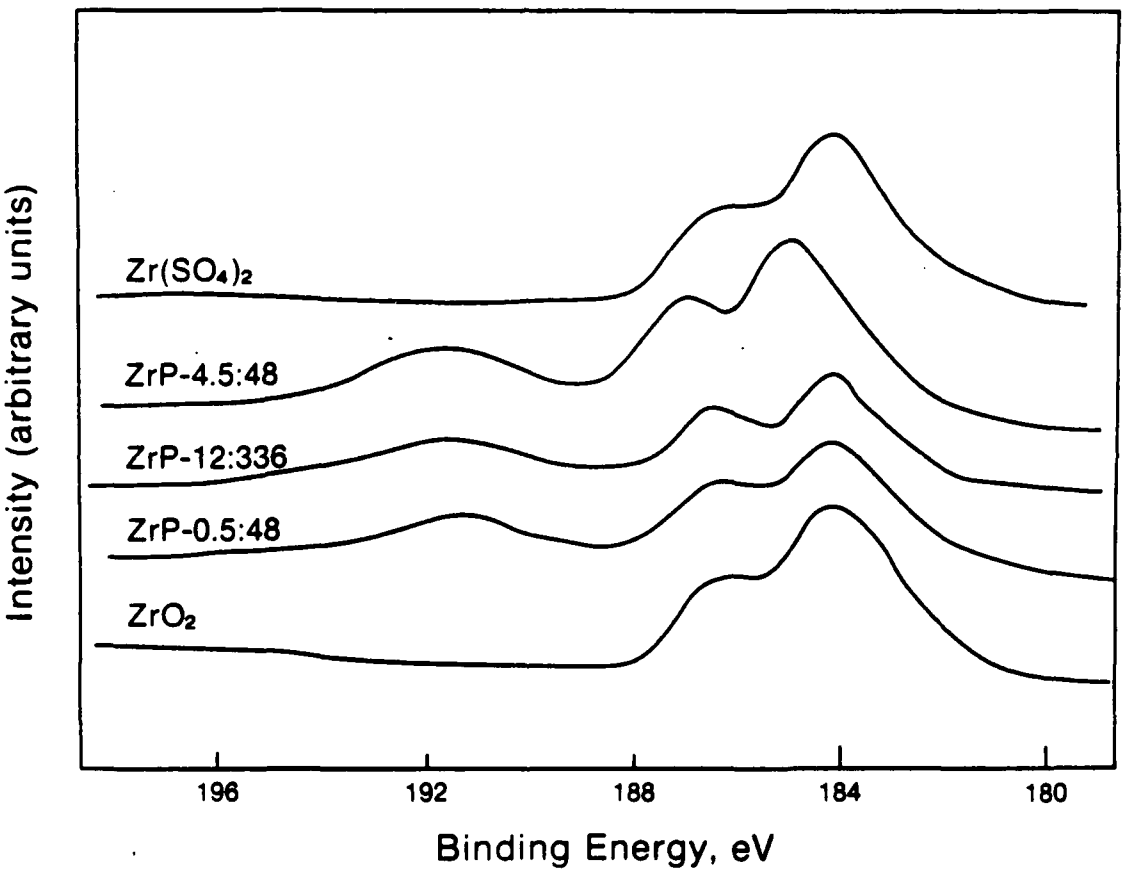
Intensity (arbitrary units)
Zr(SO4)2
ZrP-4.5:48
ZrP-12:336
ZrP-0.5:48
ZrO2
196
192
188
184
180
Binding Energy, eV

Figure 4

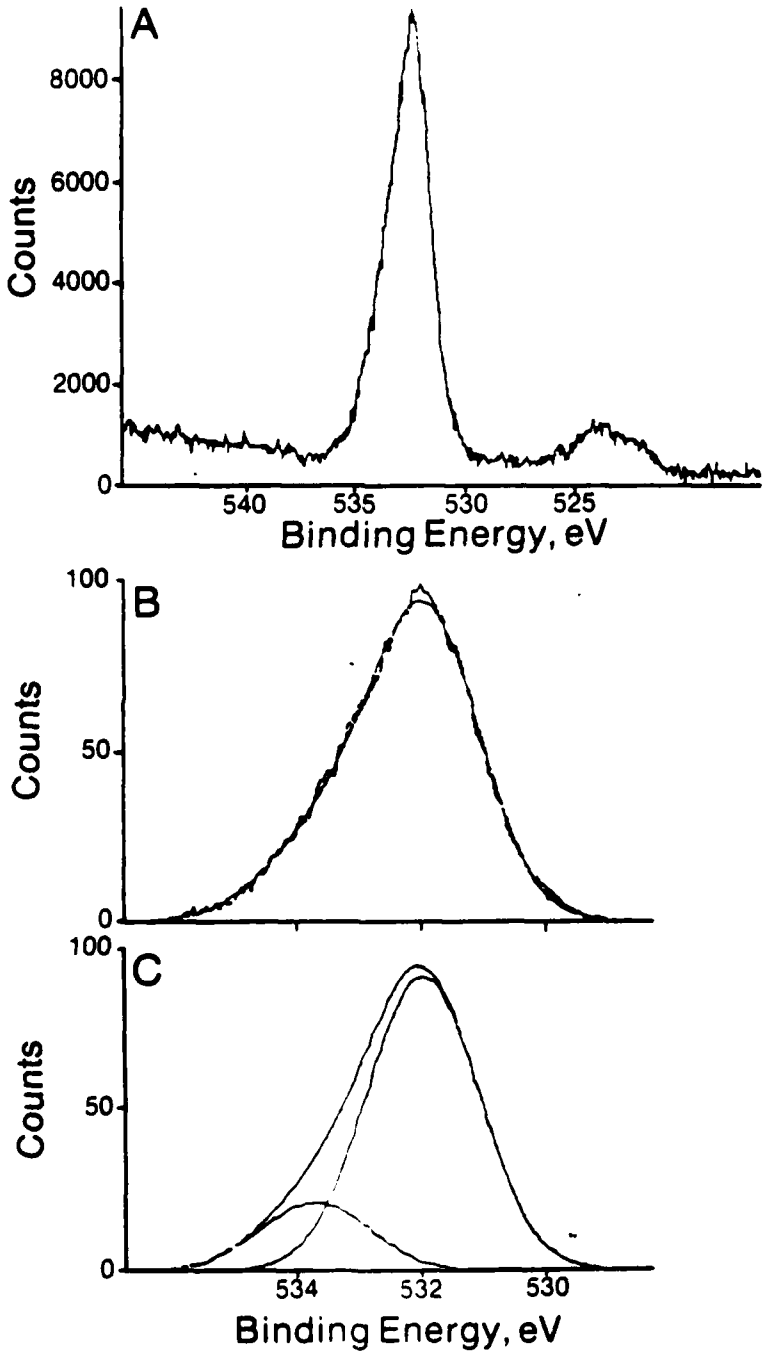
A
8000
6000
4000
2000
0
Counts
540
535
530
525
Binding Energy, eV
B
100
50
0
Counts
C
100
50
0
Counts
534
532
530
Binding Energy, eV

Figure 5

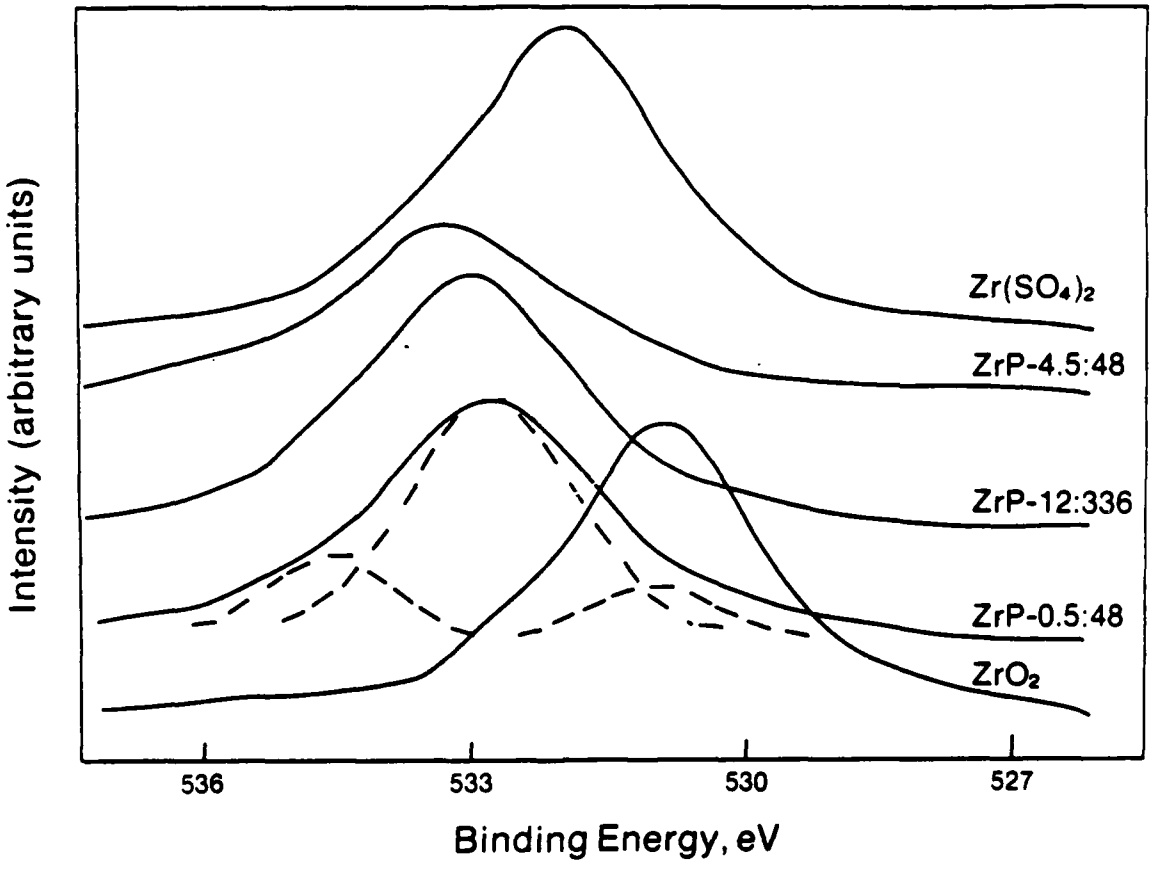
Intensity (arbitrary units)
Zr(SO4)2
ZrP-4.5:48
ZrP-12:336
ZrP-0.5:48
ZrO2
536
533
530
527
Binding Energy, eV

Figure 6

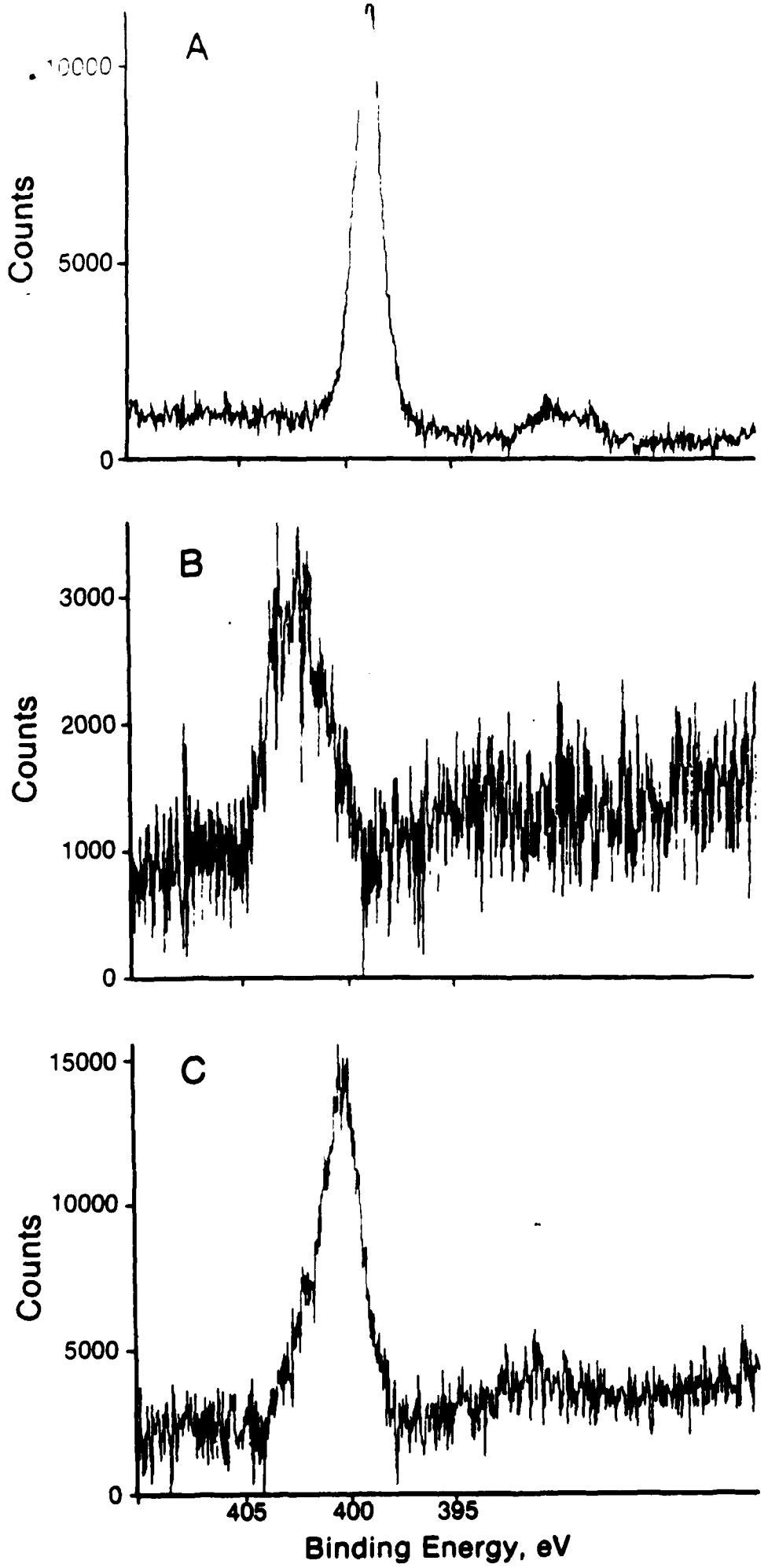
A
10000
5000
0
Counts
B
3000
2000
1000
0
Counts
C
15000
10000
5000
0
Counts
405
400
395
Binding Energy, eV

Figure 7

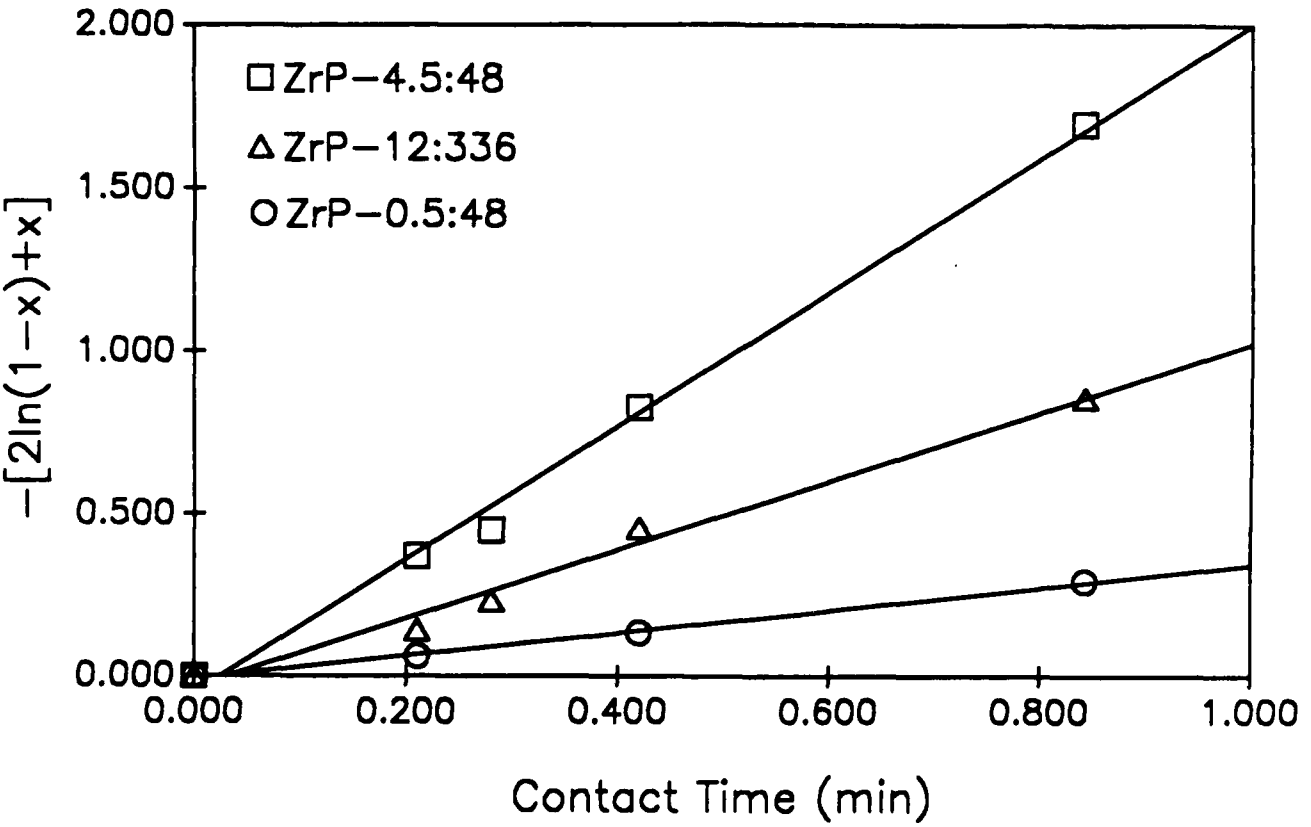
2.000
1.500
1.000
0.500
0.000
-[2ln(1-x)+x]
ZrP-4.5:48
ZrP-12:336
ZrP-0.5:48
0.000
0.200
0.400
0.600
0.800
1.000
Contact Time (min)

Figure 8

A

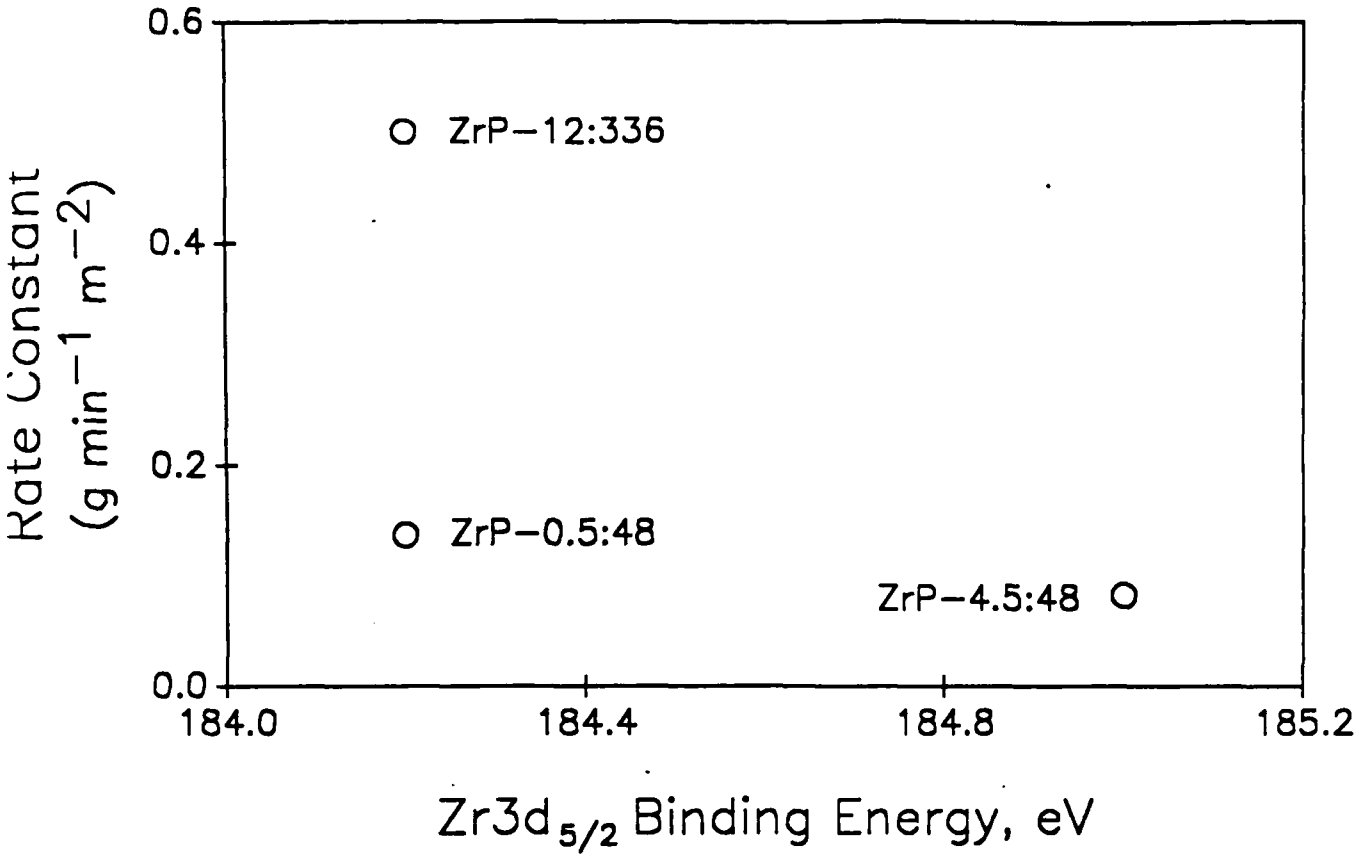
0.6
0.4
0.2
0.0
ZrP−12:336
ZrP−0.5:48
ZrP−4.5:48
184.0
184.4
184.8
185.2
Rate Constant
(g min−1 m−2)
Zr3d5/2 Binding Energy, eV

B

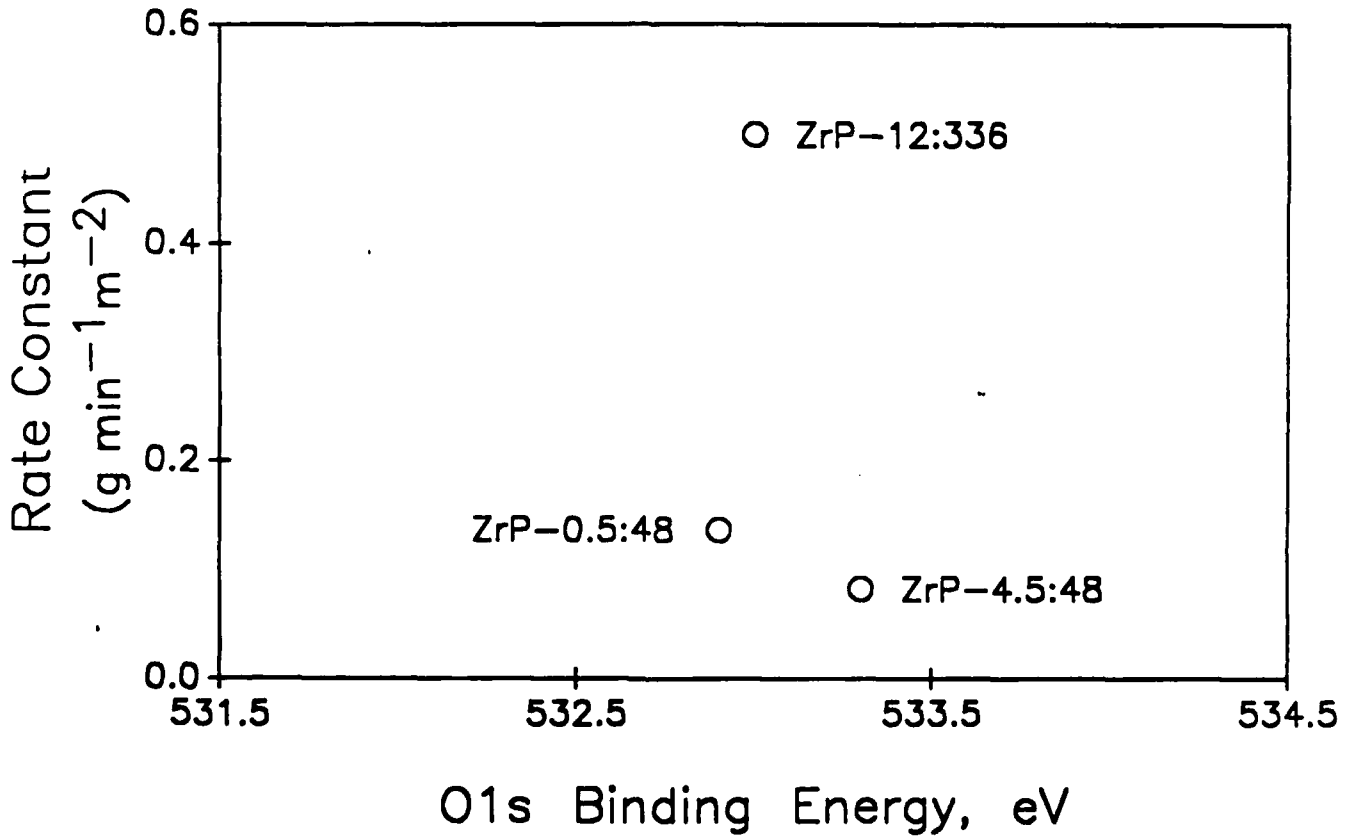
0.6
0.4
0.2
0.0
ZrP−12:336
ZrP−0.5:48
ZrP−4.5:48
531.5
532.5
533.5
534.5
Rate Constant
(g min−1m−2)
O1s Binding Energy, eV

Figure 9